Human Multidrug Resistance 3–P-Glycoprotein Expression in Transgenic Mice Induces Lens Membrane Alterations Leading to Cataract

Irene Dunia,* Jaap J.M. Smit,‡ Martin A. van der Valk,§ Hans Bloemendal,‖ Piet Borst,‡ and E. Lucio Benedetti*‖

*Département de Biologie Supramoleculaire et Cellulaire, Institut Jacques Monod du Centre National de la Recherche Scientifique, Université Paris VII, 75251 Paris Cedex 05, France; Divisions of ‡Molecular Biology and §Molecular Genetics, The Netherlands Cancer Institute, 1066 CX Amsterdam, The Netherlands; and ‖Department of Biochemistry, University of Nijmegen, 6525 EK Nijmegen, The Netherlands

Abstract. We have generated mice transgenic for a human multidrug resistance (*MDR*)3 mini-gene driven by a hamster vimentin promoter. The *MDR*3 gene encodes a P-Glycoprotein that resembles the mouse multidrug resistance 2 P-Glycoprotein shown to be involved in the translocation of the phospholipid phosphatidylcholine through the hepatocyte canalicular membrane (Smit et al., 1993. *Cell.* 75:451–462). The vimentin promoter drives expression of the *MDR*3 transgene in mesenchymal tissues and in the eye lens. We show here that the presence of human multidrug resistance 3 P-Glycoprotein in the lens results in a severe lenticular pathology. Lens structural abnormalities initiate at a late embryonic stage and increase during postnatal lens development. Differentiation of the primary fibers is affected, and the terminal differentiation of the lens epithelium into secondary fibers is also perturbed. The ultrastructural alterations, particularly of the lens plasma membranes, resemble those identified in congenital mouse osmotic cataract.

P-GLYCOPROTEINS (Pgp)[1] are highly conserved membrane proteins that can function as ATP-dependent efflux pumps (23, 31, 57). They belong to the family of ATP-binding cassette transporter proteins (37). Two genes for Pgps have been identified in humans: human multidrug resistance gene (*MDR*)1 and *MDR*3 (also called *MDR*2 [10, 72, 73], and three in mice: mouse multidrug resistance gene (*mdr*)1 (or *mdr*1b), *mdr*3 (or *mdr*1a), and *mdr*2 (16, 33, 35).

The human multidrug resistance (MDR)1 Pgp (and the related murine mdr1 and mdr3, and hamster pgp1 and pgp2 Pgps), can extrude a wide range of hydrophobic drugs from mammalian cells (18, 34, 42, 70). Increased levels of these proteins in cancer cells result in MDR. Defense against naturally occurring xenobiotic (toxic) compounds may represent the main physiological function of these Pgps (60). Attempts to show that the human MDR3 or the closely related mouse mdr2 Pgp (91% identity at the amino acid level) can confer MDR have been negative thus far (5, 35, 58, 73).

To find a physiological function for this class of Pgps, we have generated mice that are either unable to make the mdr2 Pgp or overproduce the MDR3 Pgp in many tissues (64; Smit, J.J.M., F. Baas, J.E. Hoogendijk, G. Jansen, F. Jennekens, M.A. van der Valk, A.H. Schinkel, A.J.M. Berns, K. Nooter, and P. Borst, manuscript in preparation). Mice homozygous for a disrupted *mdr*2 gene develop liver disease. A detailed analysis of these mice has shown that the mouse mdr2 Pgp (and presumably therefore also its human MDR3 counterpart) is essential for translocating phosphatidylcholine through the hepatocyte canalicular membrane into the bile (64, 65). This indicates that this Pgp is a specific phospholipid translocator, as has recently been supported by in vitro experiments (54, 66).

We have generated mice containing an *MDR*3 minigene under the control of a vimentin promoter which drives the expression of the transgene in mesenchymal tissues and in the eye lens. These mice develop a peripheral neuropathy and microphthalmia. Here we present an analysis of the abnormalities in the lenticular cells of these

Address all correspondence to E.L. Benedetti, Department of Biochemistry, University of Nijmegen, Adelbertusplein 1, 6525 EK Nijmegen, The Netherlands. Tel.: 31-80-61-67-55/61-42-54. Fax: 31-80-54-05-25.

1. *Abbreviations used in this paper:* EF, external fracture face; FVB; Friend Virus B; gapdh, glyceraldehyde-3-phospate dehydrogenase; IMP, intramembranous particles; *MDR*, human multidrug resistance gene; *mdr*, mouse multidrug resistance gene; MDR/mdr, multidrug resistance (human/mouse); PF, protoplasmic fracture face; Pgp, P-Glycoprotein.

mice during embryonic, newborn, and adult life. Immunocytochemical and ultrastructural observations show that the expression of the transgene product progressively induces cell membrane alterations that resemble those known to perturb the control of the vectorial electrochemical gradient across the lens. As a consequence, a postnatal cataract develops that may be osmotic in nature.

Materials and Methods

Transgenic Mice

We have generated mice containing an *MDR3* mini-gene under the control of a vimentin promoter which drives the expression of the transgene in mesenchymal tissues and in the eye lens. In this study, we have examined lenses from mice of the transgenic Friend Virus B (FVB) strains VO1 and VO4. Control lenses were either selected from wild-type offspring obtained from the same litter as the transgenic offspring or from mating of the wild-type FVB mouse strain.

Lens Samples

Embryos were obtained from crosses of VO1 and VO4 transgenic mice with wild-type FVB mice. Animals were mated overnight, and those with vaginal plugs were separated the following morning, which was considered to be gestational day 1 (E1). Pregnant mice were killed on E12 and E14, and the complete eyes were dissected from the embryos. Lenses or intact eyes from newborn (1–8 d after birth) and adult mice (between 2 wk and 4 mo old) were also examined. The material was rapidly fixed by immersion in cold (−20°C) 100% acetone or methanol, or in 3% paraformaldehyde in PBS, pH 7.4, at 4°C for 1 h.

For cryosectioning, the dissected lenses or the whole eyes were washed in PBS and impregnated in 2.3 M sucrose-PBS overnight at 4°C. Samples were frozen and subsequently stored in liquid nitrogen. Cryosections of 1 μm were made at −85°C with the Ultracut E (Reichert Jung S.A., Rueil, France) equipped with an FC4D cryoattachment as described by Tokoyasu (68).

Antibodies

We used affinity-purified rabbit polyclonal antibodies (polyvim K34) directed against vimentin (53) at 1:200 dilution (Organon Teknica, Turnhout, Belgium); rabbit polyclonal antibodies directed against the major intrinsic membrane protein of the lens fibers (MP26) at 1:500 dilution (19); mouse mAb C219, recognizing an epitope present in all human and mouse Pgps, at 1:100 dilution (28, 65); and affinity-purified rhodamine-labeled donkey secondary antibodies directed against rabbit and mouse IgG (Jackson ImmunoResearch Laboratories, Inc., West Grove, PA). For immunogold labeling, we used as secondary antibodies goat anti-mouse IgG conjugated to 5- or 10-nm gold particles (Amersham International, Little Chalfont, UK), or protein A conjugated to 10-nm gold particles (Department of Cell Biology, University of Utrecht, The Netherlands).

RNA Analyses

Total RNA from tissues was isolated by acidic guanidinium isothiocyanate-phenol-chloroform and was analyzed by RNase protection as described (64). The plasmid construct for detection of *MDR3* contains a 310-nucleotide HindII–TaqI fragment (64). For detection of glyceraldehyde-3-phosphate dehydrogenase (*gapdh*) mRNA, a 146-bp BsteII–HindIII fragment from pmGAP was blunted and cloned in a SmaI site of pGEM3-Zf(−). To synthesize antisense RNA probes, we linearized the plasmid templates with BamHI (*gapdh*) and HindIII (*MDR3*), and transcribed them with T7 RNA polymerase. ^{32}P-labeled RNA transcripts were hybridized with 10 μg of total RNA from the tissue of interest. The protected probe was visualized by electrophoresis through a denaturing 6% gel, followed by autoradiography.

SDS-PAGE and Immunoblotting

Decapsulated lenses of control and transgenic mice were homogenized in 40 mM KCl, 2 mM $MgCl_2$, and 50 mM Tris-HCl, pH 7.5 (TKM buffer), containing 2 mM PMSF. After two washes in TKM buffer, the plasma membrane–cytoskeleton complex obtained by centrifugation at 3,000 *g* for 10 min was subsequently treated with 4 M urea for 15 min. The urea-insoluble material was collected by centrifugation at 100,000 *g* for 45 min. SDS-PAGE was carried out in 12 and 10% polyacrylamide slab gels according to Laemmli (see also 20) using a miniprotean II slab cell (Bio-Rad Laboratories, Richmond, CA) operating at 180 V for 1 h. Aliquots of the different samples were solubilized in sample buffer (2% SDS, 5% 2-β-mercaptoethanol) without heating. After electrophoresis, the gels were stained with Coomassie blue.

Proteins separated by SDS-PAGE were electrophoretically transferred onto nitrocellulose paper and incubated with the primary antibodies as described (20). Alkaline phosphatase–conjugated or HRP-labeled goat anti-mouse or anti-rabbit IgG were used as secondary antibodies (Promega Biotec, Madison, WI). For alkaline phosphatase–conjugated antibodies, the color reaction was developed with 5-bromo-4-chloro-3-indolyl phosphate/nitroblue tetrazolium (BCIP/NBT kit; Kirkegaard & Perry Laboratories, Inc., Gaithersburg, MD). For HRP-labeled antibodies, enhanced chemiluminescence detection was performed (ECL kit; Amersham International).

Immunofluorescence

Immunofluorescence experiments were performed on 1-μm cryosections, placed onto poly-L-lysine–coated coverslips. Sections were fixed with 3% paraformaldehyde-PBS for 10 min, thoroughly washed in PBS, and incubated in a quenching solution of 50 mM NH_4Cl-PBS for 20 min and in a blocking solution (PBS-0.2% gelatin) for 30 min. Immunolabeling was performed by incubating the sections consecutively in the primary and in the rhodamine-labeled secondary antibodies for 45 min. 0.2% gelatin-PBS solution was used for antibody dilutions and washes. Nuclei of cells were stained with 4,6-diamidino-2-phenylindole, 0.1 mg/ml in PBS, for 5 min. Sections were mounted using Mowiol (Hoechst, Frankfurt, Germany) and examined with a microscope (Aristoplan; E. Leitz, Inc., Wetzlar, Germany) equipped with epifluorescence illumination and with ×63 NA 1.4 and ×100 NA 1.32 immersion optics.

Confocal Laser Scanning Microscopy

Confocal laser scanning microscopy was performed using an MRC-600 (Bio-Rad Laboratories) mounted on a microscope (Optiphot II; Nikon Inc., Garden City, NY) equipped with a ×60 objective (plan apochromatic NA 1.4), on 2.5-μm cryosections processed for immunofluorescence as described before. For rhodamine, a helium-neon ion laser adjusted at 543 nm was used, close to the maximum of absorption. The signal was treated by Kalman filter (average eight images), and the pinhole of the confocal system was adjusted to allow a field depth of ~0.6 μm. A focal series of up to 10 sections apart was collected for each specimen and then processed to produce single composite images (extended focus) with high spatial resolution.

Photographs were taken on film (Kodak T-Max; Eastman Kodak Co., Rochester, NY) using a camera mounted on a film recorder (VM-1710; Lucius & Baer, Geretsried, Germany).

Histological Sections

Lenses or intact eyes were fixed overnight in a mixture of 0.25% glutaraldehyde and 3% paraformaldehyde-PBS at 4°C. After washing in PBS, the samples were dehydrated in a series of graded ethanol solutions and embedded in LR white. 1.5-mm semithin sections were placed onto poly-L-lysine–coated slides, dried, stained with 1% toluidine blue, and examined with a Leitz Aristoplan microscope.

Electron Microscopy

Four thin-section EM lenses were fixed in 2% glutaraldehyde in 0.2 M cacodylate buffer, pH 7.4, for 1 h, washed in the same buffer, and subsequently fixed in a mixture of 1% osmium tetroxide/0.8% potassium ferrocyanate in the same buffer for 40 min. After washing, the samples were dehydrated in a series of graded ethanol solutions and embedded in Epon Araldite. Thin sections were stained with uranyl acetate and lead citrate.

Immunogold labeling was performed on 1-μm cryosections of 3% paraformaldehyde– or methanol-fixed intact tissue with the same protocol described for immunofluorescence, using as secondary antibodies the cor-

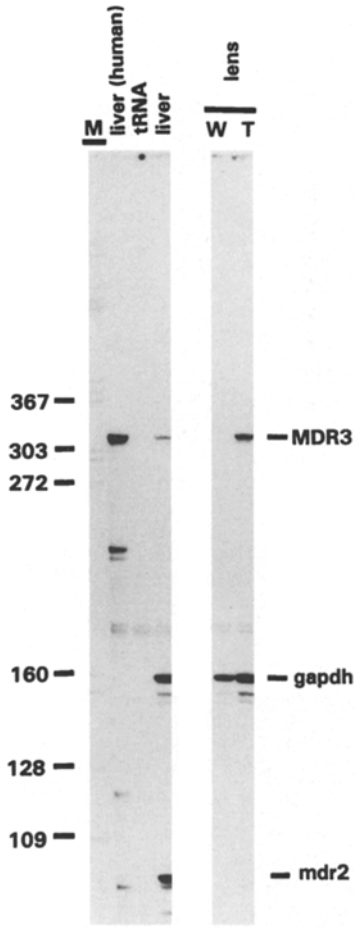

Figure 1. The level of *MDR3* mRNA in the transgenic lens. Total RNA was isolated from the lenses of transgenic (*T*) V01 animals or wild-type (*W*) animals and analyzed by RNase protection. The protected fragments representing *MDR3*, *mdr2*, and *gadph* mRNA are indicated on the right side. For comparison, an analysis of *MDR3* expression levels in RNA isolated from a human liver and a V01 transgenic mouse liver. Due to the partial sequence homology of the *MDR3*-specific RNA probe with mouse *mdr2* sequences, a smaller fragment was detected that represents *mdr2* mRNA in RNA from liver. As size marker (*M*), an end-labeled DdeI digest of M13mp19 DNA was used; relevant sizes are indicated at the left.

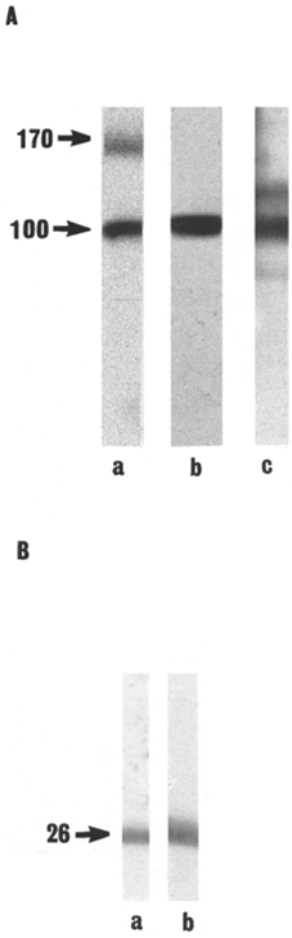

Figure 2. (*A*) Immunoblot analysis of urea-insoluble lens plasma membrane fractions from newborn transgenic mouse lenses (lane *a*) and of cataractous adult transgenic mouse lenses (lane *b*). For comparison, an urea-insoluble fraction of eye tissue of a control mouse after removal of the lens (lane *c*). Protein blots were incubated with the Pgp-reactive mAb C219. Detection was done by chemiluminescence. (*B*) Immunoblot analysis of urea-insoluble lens plasma membrane fractions from control lenses (lane *a*) and from cataractous transgenic mouse lenses (lane *b*). Protein blots were incubated with the polyclonal antiserum against MP26. Detection was achieved by an alkaline phosphatase–based method.

responding gold conjugates. The immunogold-labeled cryosections were postfixed in 2% glutaraldehyde in 0.2 M cacodylate buffer for 30 min and in 1% osmium tetroxide in the same buffer for 45 min, and then processed for thin sections as described before. To favor the immunogold labeling, some cryosections were fixed with 1.5% paraformaldehyde for 20 min, extracted for 5 min with 1% Triton X-100 in PBS, postfixed with 100% cold methanol (−20°C), and then processed for immunogold labeling. Other lens samples were extracted with 1% Triton X-100 in TKM, after repeated washing in the same buffer, fixed in 1.5% paraformaldehyde for 20 min, and processed for cryosectioning and immunogold labeling using the C219 antibody. After the latter step, the cryosections were embedded either in Epon or in LR white. Thin sections of this material were stained with uranyl acetate.

For freeze fracturing, small pieces of the 2% glutaraldehyde–fixed lenses were washed in PBS and gradually impregnated with 30% glycerol/PBS overnight at 4°C. Each piece was mounted in a specimen holder, rapidly frozen in Freon 22, (Dehon, Paris, France) and stored in liquid nitrogen. Freeze fracturing was performed at −120°C or at −150°C in a freeze-fracture apparatus (model 301; Balzers, Liechtenstein). After fracture, the specimens were immediately shadowed by platinum/carbon evaporation from an electron gun.

Thin sections and freeze-fracture replicas were examined with an electron microscope (EM 400 or EM 410; Philips, Eindhoven, Holland) operating at 80 kV.

Chemicals

Unless otherwise indicated, all chemicals used for this work were purchased from Sigma Chemical Co. (St. Louis, MO).

Results

Generation of Mice Transgenic for the Human MDR3 Gene

Several transgenic mice strains (VO1 to VO8), have been generated (Smit et al., manuscript in preparation) by injecting an *MDR3* P-glycoprotein mini-gene under the control of the hamster vimentin promoter into fertilized mouse oocytes. This promoter drives the expression of the transgene in all tissues in which the vimentin gene is normally expressed, i.e., in tissues of mesenchymal origin and in the eye lens (52).

Detection of MDR3 RNA and MDR3 Pgp in Transgenic Lens Extracts

We have previously shown that immortalized transgenic fibroblast cells derived from the VO1 mouse strain contain a high level of *MDR3* mRNA which is translated into full-length MDR3 Pgp and routed to the plasma membrane

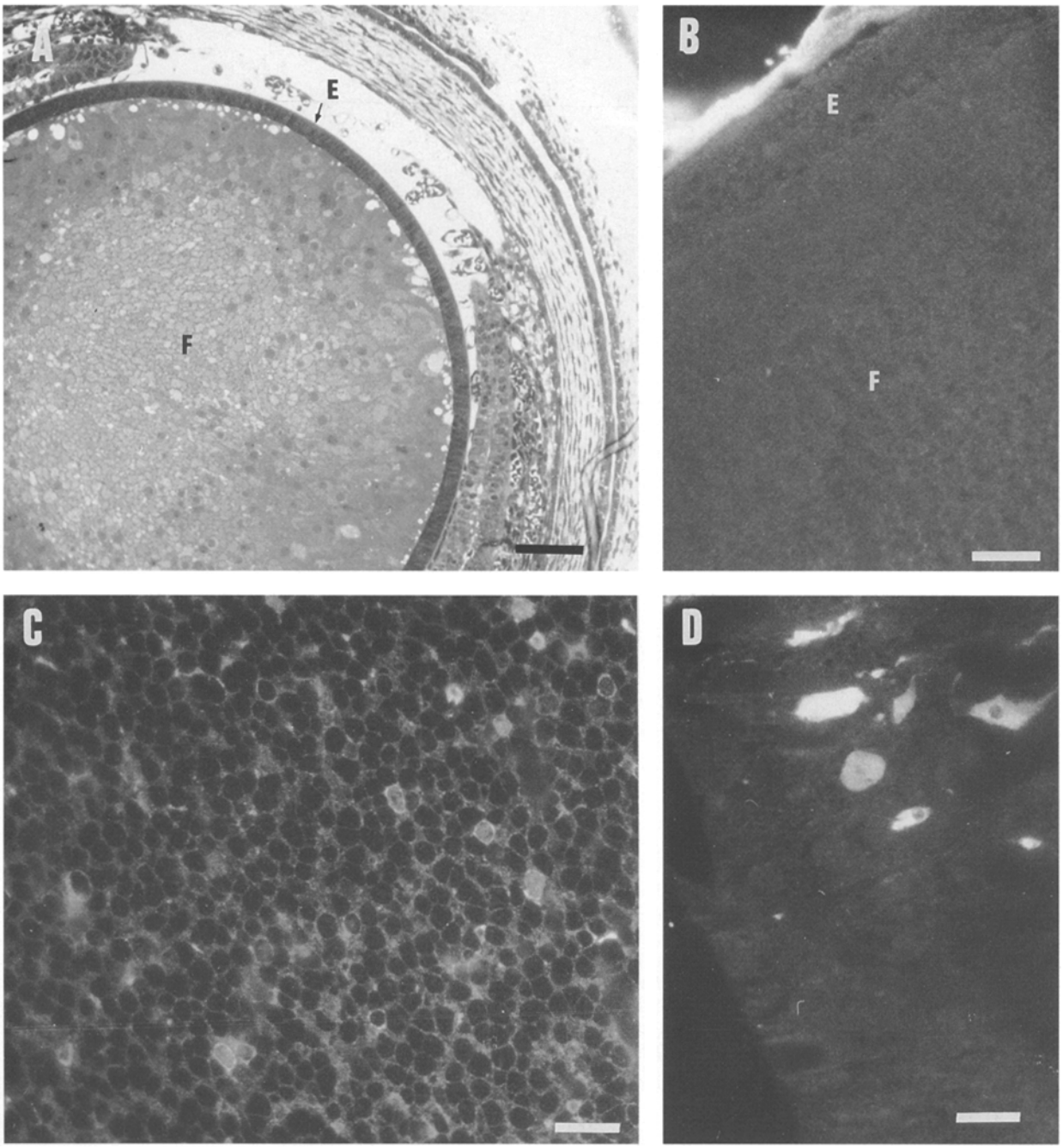

Figure 3. (*A*) Histological section (LR white) of transgenic mouse embryonic eye (day 14). Note the normal organization of the lens primary fibers (*F*), the lens anterior epithelium (*E*), and all other ocular tissues. Bar, 300 μm. (*B*) Cryosection of a control embryonic eye (day 14), incubated with the Pgp-reactive mAb C219. Note the presence of highly fluorescent ocular connective-tissue derivatives surrounding the lens. In contrast, the lens appears completely negative. *E*, epithelium; *F*, primary fibers. Bar, 125 μm. (*C* and *D*) Cryosections of transgenic mouse embryonic lenses (day 14) incubated with the C219 antibody. MDR3-Pgp is present only in a few randomly scattered primary fibers. Bars: (*C*) 150 μm; (*D*) 200 μm.

(59, 65). Fig. 1 shows that *MDR3* mRNA can be detected in the lens of newborn transgenic mice, but not in that of control mice. In agreement with these results, a protein migrating at ~170 kD, the relative mobility of full-length glycosylated MDR3 Pgp (58), was detected in immunoblots of isolated lens plasma membranes from newborn transgenic mice (Fig. 2 *A*, lane *a*), but not from control mice (not shown). The C219 antibody used in these experiments reacts with all human and murine Pgps. No 170-kD band was found in samples of isolated plasma membranes from adult cataractous transgenic lenses (Fig. 2 *A*, lane *b*), but instead there was a prominent band at 100 kD, which was also present in other lanes in Fig. 2 *A*. Several bands ranging from ~80 kD to 150 kD were recognized by C219 in immunoblots of control mouse ocular tissues after removal of the lens (Fig. 2 *A*, lane *c*). Whether these bands are due to Pgp degradation products or cross-reacting proteins remains to be established.

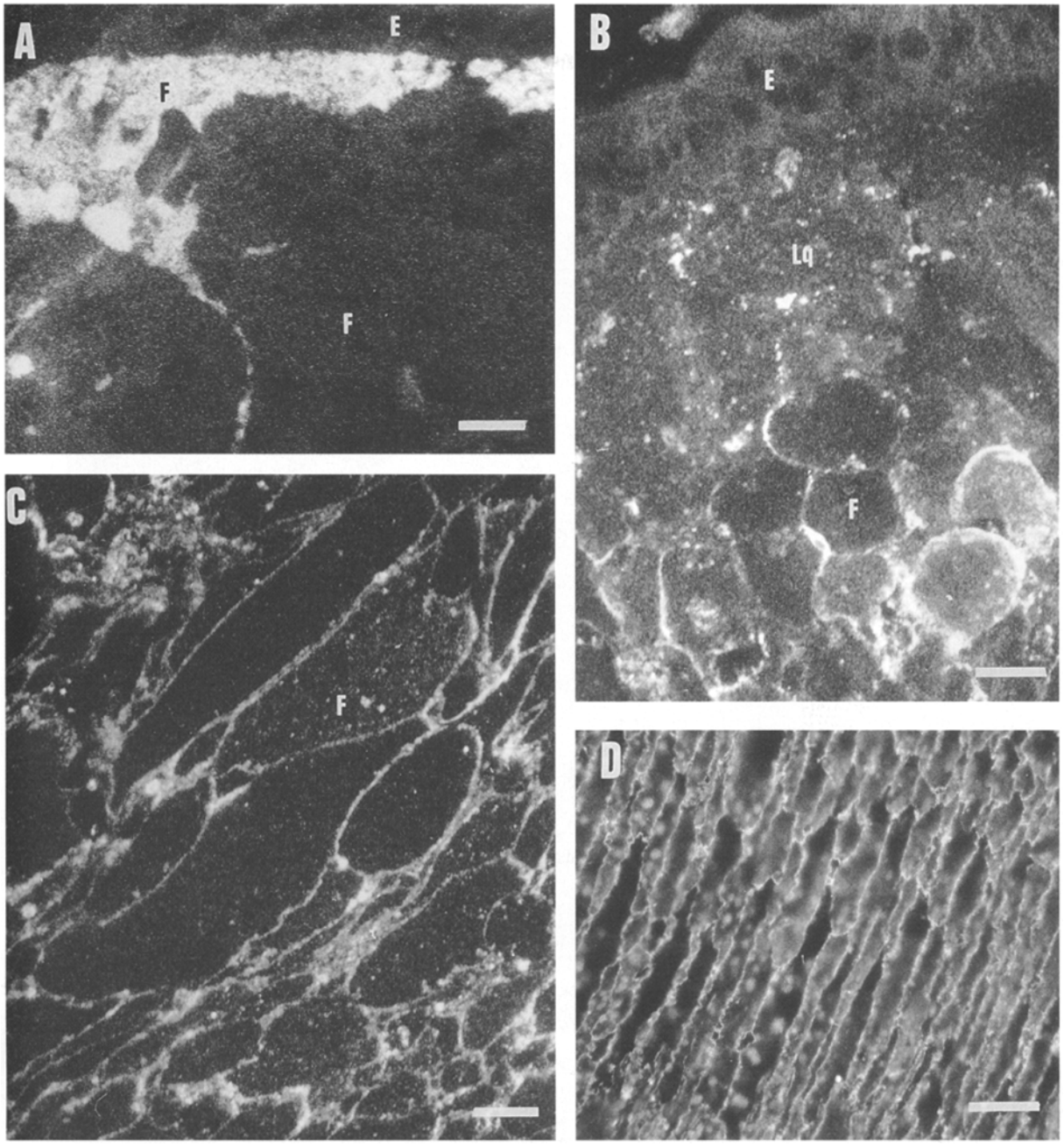

Figure 4. (*A*) Confocal laser scanning microscopy on a cryosection of newborn transgenic mouse lens incubated with the C219 antibody. The MDR3 expression appears distributed in a mosaic fashion, particularly in the lens fibers (*F*) lying underneath the anterior epithelium (*E*). Bar, 100 μm. (*B* and *C*) Confocal laser scanning microscopy on cryosections of newborn transgenic mouse lenses incubated with an MP26 antibody. Note the great variety of shape and orientation of the fibers (*F*) outlined by the intense fluorescence of the membrane profiles. The fibers (*F*) lying underneath the epithelium (*E*) are no longer detectable, and areas of liquefaction (*Lq*) are visible in regions where MP26 forms clusters of intensely fluorescent granular material. Bar, 100 μm. (*D*) Confocal laser scanning microscopy on cryosection of control newborn mouse lens incubated with MP26 antibody. The typical aspect and regular pattern of the fiber membrane profiles are outlined by the antibody. Bar, 200 nm.

Immunoblots stained with the antibody raised against MP26, the major intrinsic membrane protein of the lens fibers, indicate that the isolated fiber plasma membranes, after 4 M urea extraction, contain MP26 but not its degradation product, MP22. This pattern is present in the isolated plasma membranes from newborn (not shown) and adult cataractous lenses of transgenic mice (Fig. 2 *B*).

Gross Defects in Eyes of Transgenic Mice

The shape, size, and transparency of lenses from E12–E14 transgenic embryos were comparable to those of control mice, but in newborns the transgenic lenses were smaller and softer than in controls. Adult mice developed microphthalmia. Histological sections revealed that the rem-

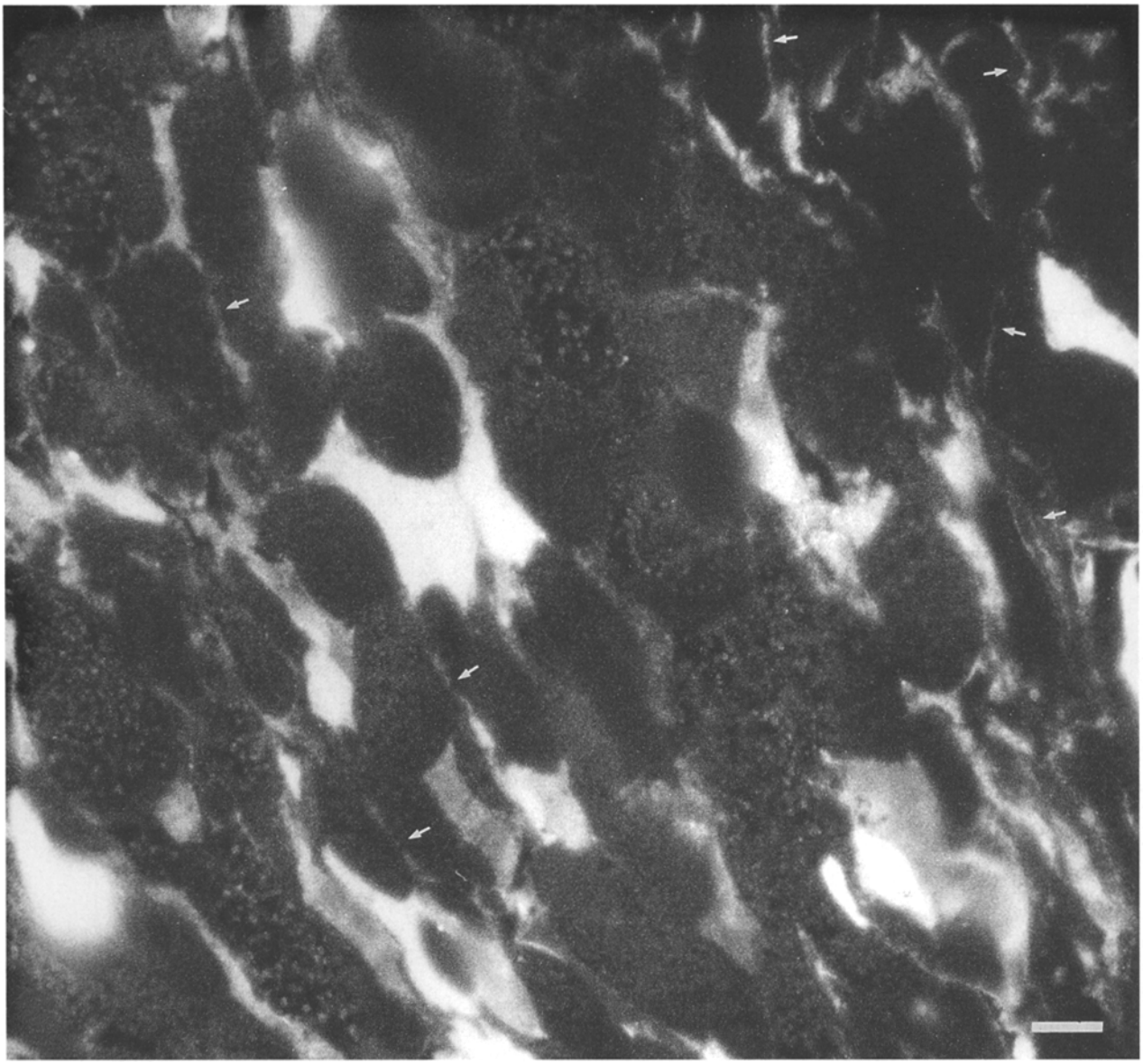

Figure 5. Cryosection of newborn transgenic mouse lens incubated with C219 antibody. Elongating fibers display uneven distribution of the transgene product which appears in a mosaic fashion. Note the presence of highly fluorescent material either filling the fibers or outlining the membranes (*arrows*). Bar, 50 μm.

nant lens appeared more like a bladder than a compact cellular mass (see also Fig. 8 *A*).

Immunocytochemistry of Embryonic Lenses

In Fig. 3 *A*, the normal cell organization of the transgenic embryonic lens is shown. The C219 antibody stains a few randomly scattered cells (mainly primary fibers) in the transgenic lens (Fig. 3, *C* and *D*), but not in control lenses (Fig. 3 *B*). In addition, other eye tissues are intensely stained with C219, both in the transgenics and controls (Fig. 3 *B*). This may be due to endogenous mouse Pgps, which are also recognized by C219.

In both transgenic and control lenses, vimentin is uniformly distributed in primary and secondary fibers and in the anterior epithelial layer. Antibodies against MP26 react with the lens fiber plasma membranes but not with the epithelium in both transgenic and control embryonic lenses (not shown).

Immunocytochemistry and Electron Microscopy of Lenses from Newborn and Adult Transgenic and Control Mice

In newborn transgenic mouse lenses, the MDR3-Pgp detected by fluorescence with the C219 antibody is dramatically increased in comparison with the embryonic stages. However, the expression is still not uniform, but very high in some cells, whereas in others, particularly in the anterior lens epithelium, MDR3-Pgp is not detectable (Figs. 4 and 5). The MDR3-Pgp appears to be present mainly as the equatorial/epithelial cells elongate, orient themselves obliquely, and come to lie beneath the epithelium. Nucleated bow fibers are also occupied by C219-reactive material,

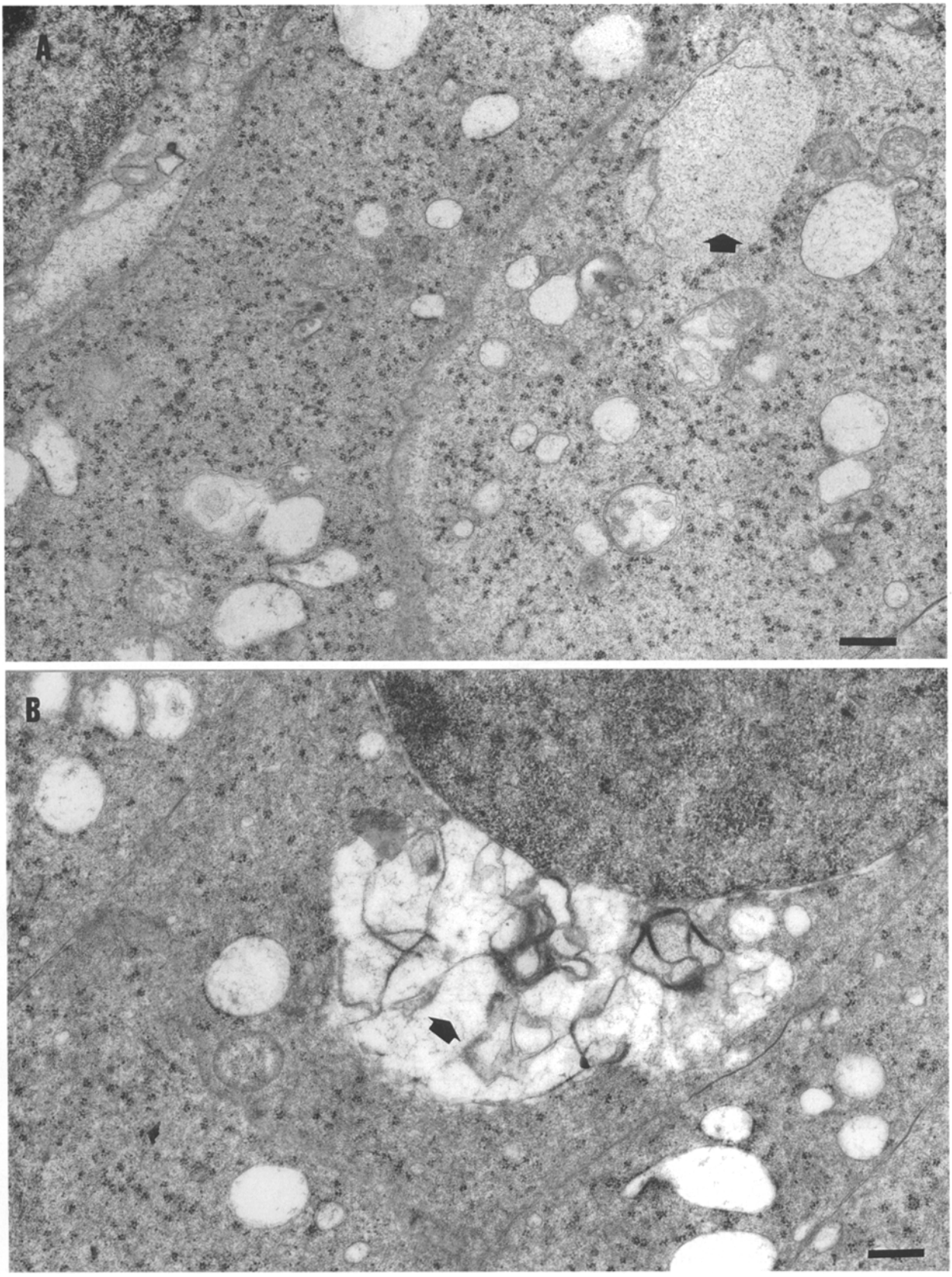

Figure 6. (*A* and *B*) Thin sections of newborn transgenic mouse lenses stained with uranyl acetate and lead citrate. The fiber cytoplasm is occupied by many vacuoles of different sizes and shapes containing either amorphous material (*A*, *arrow*) or sequestrated membrane remnants (*B*, *arrow*). Bar, 30 nm.

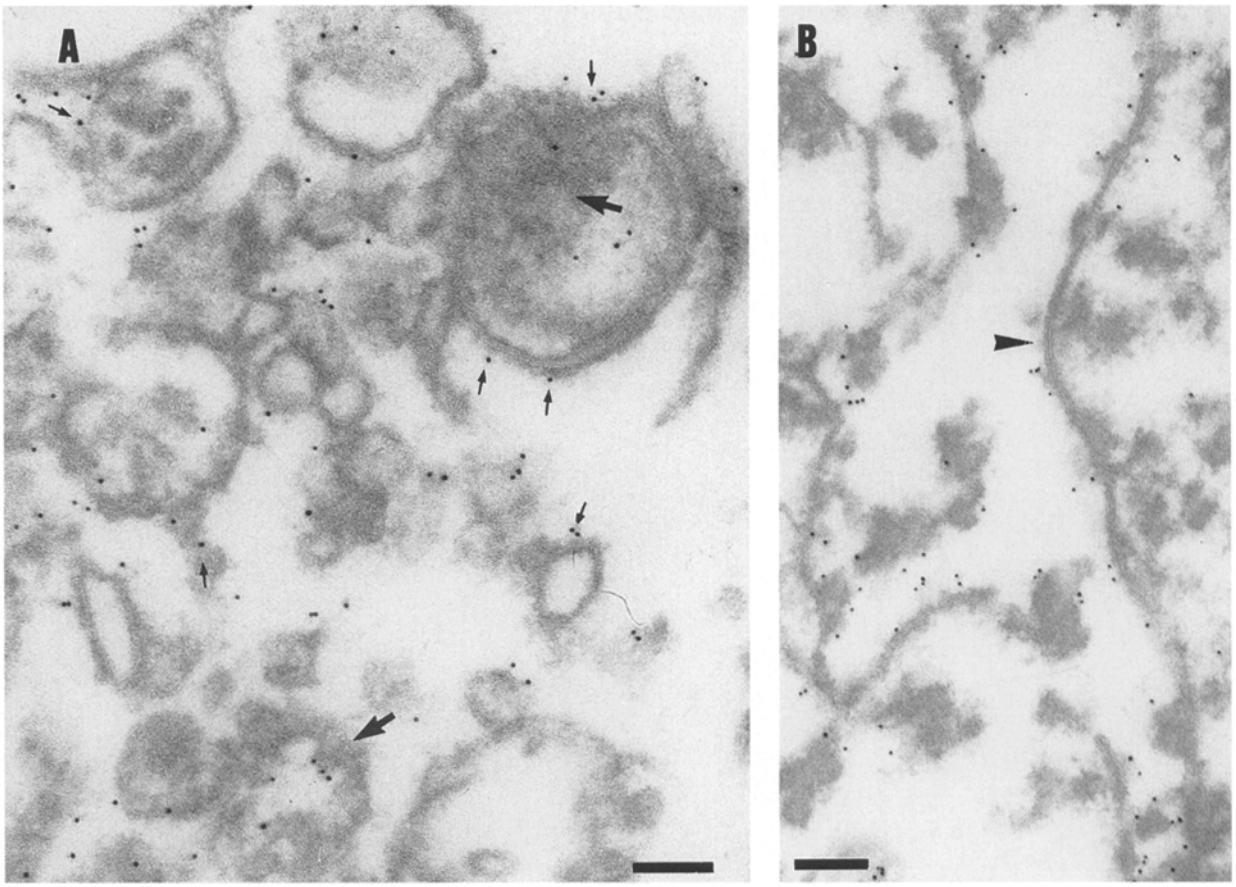

Figure 7. (*A* and *B*) Cryosections of transgenic mouse lens fragments extracted with Triton X-100 and immunogold labeled with C219 antibody. Note that the gold particles are labeling amorphous material closely attached to the cytoplasmic sides either of the vesicular profiles (*small arrows*) or of junctional complexes (*arrowheads*). Gold particles are also visualized on tangential sections going through the membrane profiles (*thick arrows*). Bars: (*A*) 120 nm; (*B*) 150 nm.

and the expression of the transgene is also evident in several primary fibers of the lenticular core (Fig. 5). Fluorescence appears either associated with amorphous cytoplasmic material or outlining the plasma membrane (Fig. 5, *arrows*). Many cells expressing *MDR*3 have a polygonal shape, while some others fuse together forming rather large cellular conglomerations underlining the anterior epithelium or the posterior capsule (Fig. 4 *A*). Using the MP26 antibody, the honeycomb arrangement, characteristic of the control lens fibers (Fig. 4 *D*), is no longer apparent. The fibers display a large variation in shape, thickness, and orientation (Fig. 4, *B* and *C*). Internalization of membrane and junction domains is also a predominant feature. In the lens regions where the C219 staining is highest, cell fusion and liquefaction are detectable. In these areas, staining with the MP26 antibody shows disruption of the plasma membranes and a granular material dispersed within the fused fibers (Fig. 4 *B*). In control newborn mice, transgene expression, monitored with the C219 fluorescence, was totally absent in all lenticular cells. Intense fluorescence was present only in the remnants of the hyaloid vascular system and in other derivatives of ocular connective tissue, as also shown in embryonic control eyes (Fig. 3 *B*).

Electron microscopic sections of newborn transgenic mouse lenses show the presence of many cytoplasmic vacuoles (Fig. 6 *A*) absent in control mice. These vesicles have different sizes and shapes and contain internalized membrane profiles and amorphous material (Fig. 6 *B*). Immunogold labeling of cryosections with the C219 antibody, particularly of Triton-extracted lens samples, shows that many gold particles are associated either with amorphous material or with internalized membranes and junctions (Fig. 7, *A* and *B*).

The advanced stages of lens pathology of adult transgenic mice are characterized by swollen fibers and ablation of the central lenticular core. The anterior and posterior sutures become undetectable, and the lens appears more like a bladder than a compact cellular suborgan (Fig. 8 *A*). The lenticular tissue is surrounded by a thick capsula. Underneath this fibrillar coat, a layer of either polygonal or elongated flattened cells is present surrounding the central cavity (Fig. 8, *A* and *C*). The cells forming the wall of the lens bladder possess a well-developed ER, mitochondria, and Golgi apparatus (Fig. 8 *C*). They contain thick bundles of vimentin intermediate filaments (not shown).

Immunocytochemistry on cryosections of adult transgenic mouse cataractous lenses, using specific antibodies against Pgp (Fig. 8 *B*) and vimentin, respectively (Fig. 8 *C*, *inset*), reveals that many cells express these proteins.

In this material, some polygonally shaped cells are characterized by a great number of surface projections and mi-

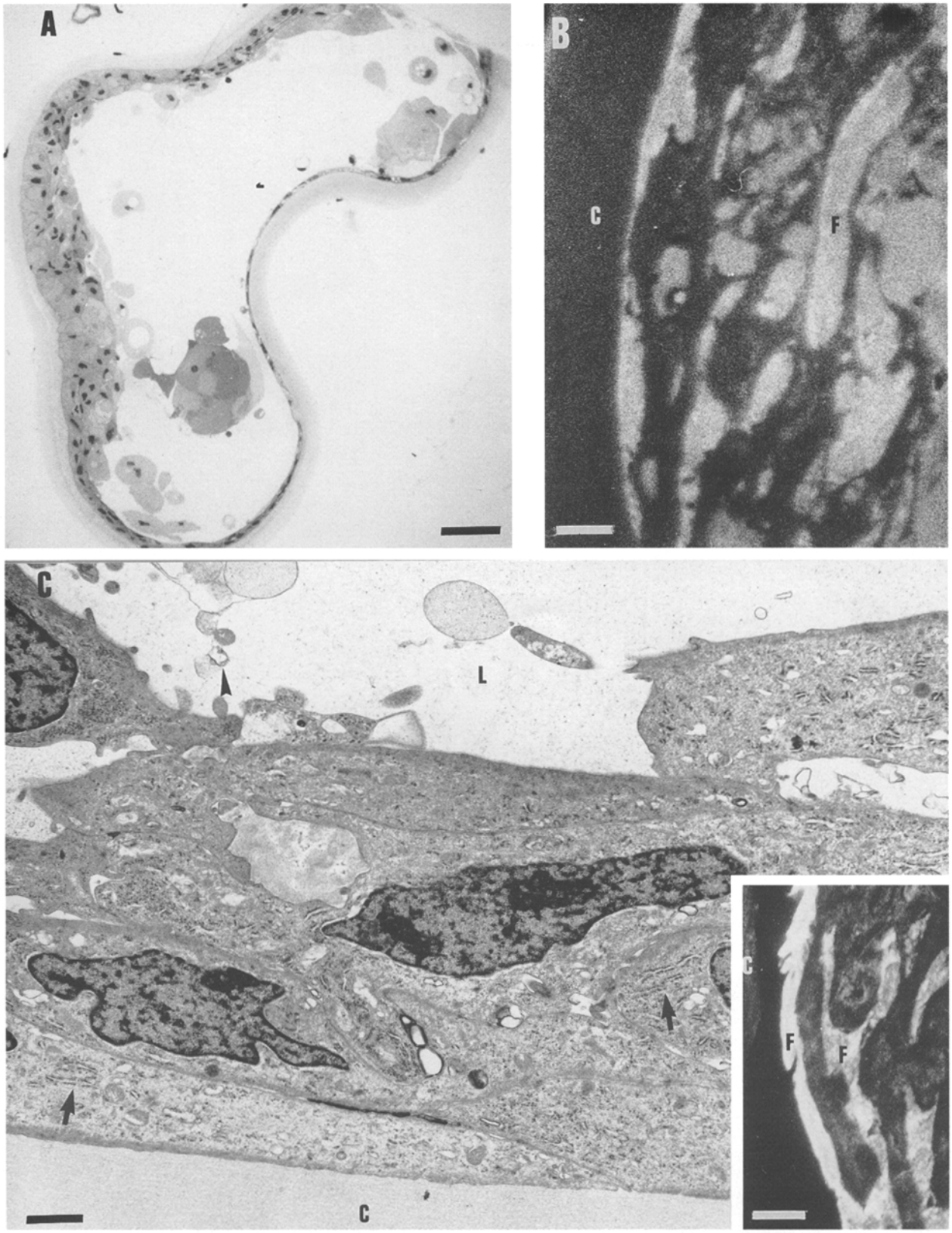

Figure 8. (*A*) Histological section (LR white) of a cataractous adult transgenic mouse lens. The lens appears as a bladder surrounded by a thick capsule and formed by multilayered, round-shaped, and elongated nucleated cells. The bladder cavity is occupied by swollen cellular debris. Bar, 150 μm. (*B*) Confocal laser scanning microscopy on cryosection of a cataractous adult transgenic mouse lens incubated with C219 antibody. Note the mosaic distribution of the transgene product highly expressed in elongated multilayered cells. Note that the capsule (*C*) is not stained. Bar, 60 μm. (*C*) Thin section of the wall of the lens bladder in a transgenic mouse adult cataractous lens, stained with uranyl acetate and lead citrate. The cells are characterized by a well-developed, rough ER (*arrows*). Note the presence of cytoplasmic vacuoles and shedded membranes (*arrowheads*). *L*, lumen; *C*, capsule. Bar, 2 μm. (*Inset*) Cryosection of the same material incubated with anti-vimentin antibody, showing the mosaic distribution of this protein. *F*, fibers; *C*, fragment of capsule detached from the lens during sectioning. Bars: (*C*) 200 nm; (*inset*) 80 μm.

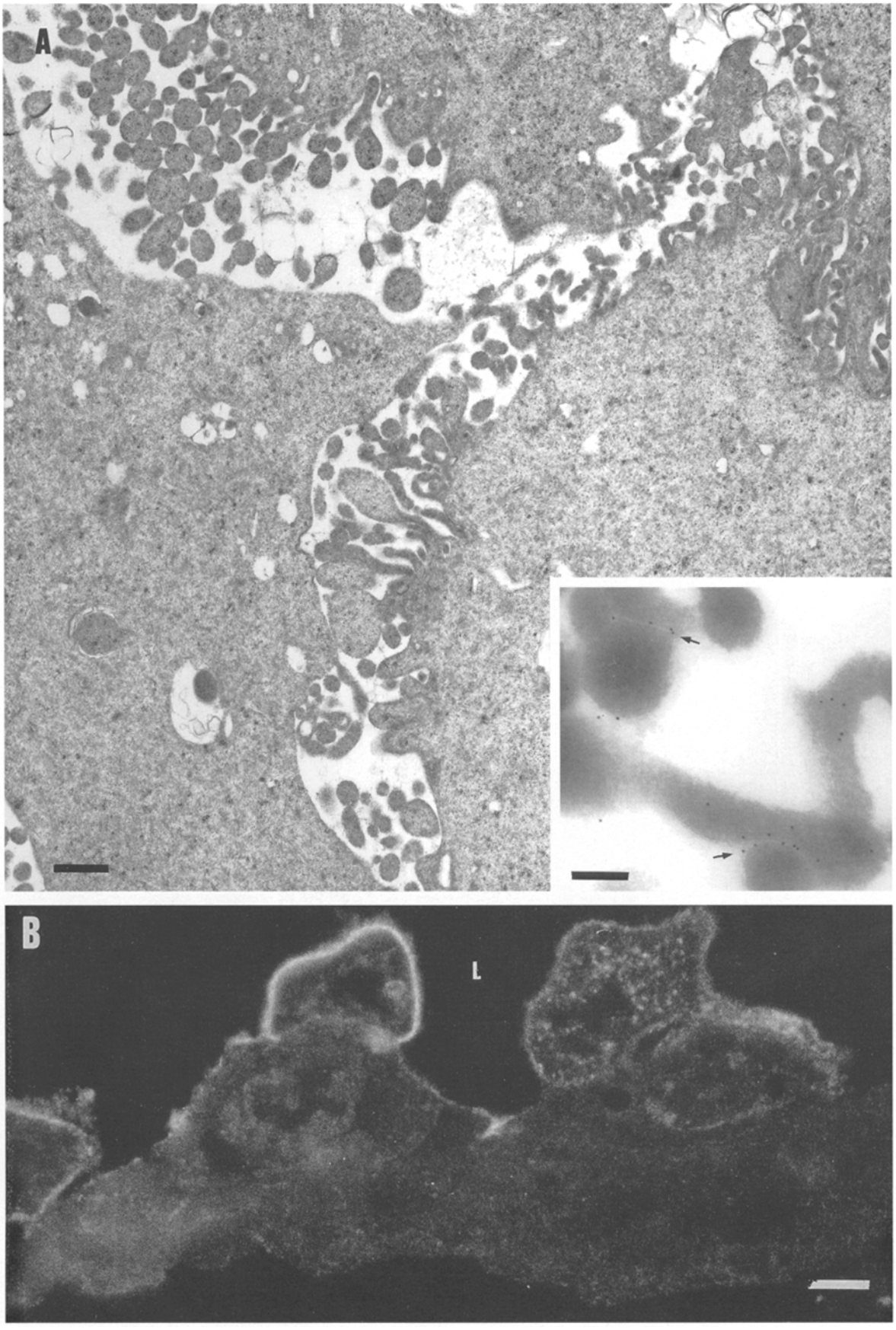
A
B
L

crovilli that occupy the intercellular space. Some of these cellular projections appear pinched off from the plasma membrane and lie as individual round or oval structures in the extracellular domain (Fig. 9 *A*). Immunofluorescence (Fig. 9 *B*) and immunogold labeling (Fig. 9 *A*, *inset*), using antibodies against MP26, show that this protein is associated with the surface of cell projections.

Freeze Fracture of Lenses from Embryonic, Newborn, and Adult Transgenic and Control Mice

Embryonic lenses of transgenic mice are characterized by freeze-fracture features comparable to those found in control mice. The intramembranous particles (IMP) of the protoplasmic fracture face (PF) and the pits, characteristic of the external fracture face (EF) of the plasma membrane, are randomly distributed (not shown).

In newborn transgenic mouse lenses, freeze fracture of the outer cortical fiber plasma membranes reveals the presence of large areas of PF occupied by tetrameric IMP forming a lattice of packed arrays (Fig. 10). Such square arrays are also present in deeper regions of the lens. In the newborn control lenses, the same arrays are only restricted to the nuclear fiber plasma membranes (not shown).

The plasma membrane of the adult cataractous transgenic mouse lens cells is characterized by an impressive accumulation of tetrameric IMP arrays on the PF, either forming randomly scattered small clusters or large square lattices of repeating subunits (Fig. 11 *A*) often interspaced by areas devoid of particles (Fig. 11 *B*). The cells forming the lenticular cataractous wall can be easily recognized because they have an elongated shape and fingerlike processes. Freeze fracture of these cells reveals that their PFs are characterized, in addition to the square arrays (Figs. 10 and 11), by the presence of 8-nm particles, exhibiting cluster distribution or forming interlaced rows (Fig. 12, *A* and *C*). Typical gap junctions are also present, being characterized by both geometrically packed arrays of 8-nm repeating subunits, or by large nongeometric assemblies of 8-nm repeating subunits (Fig. 12, *B* and *D*).

Discussion

Expression of the MDR3-Pgp in the Lens

Our results demonstrate that the human *MDR*3 gene, driven by the vimentin promoter, is expressed in lenticular cells. The level of expression, monitored by immunofluorescence, is prominent in the newborn and adult mouse lens. mAb C219, which we have used as immunoprobe, recognizes all mammalian Pgps (28), and we have shown that no Pgps are present in the normal eye lens. This fact made it possible to identify both the onset and site of production of the MDR3-Pgp in the lens and to characterize tissue alterations when the ectopic Pgp becomes expressed.

Differing from the endogenous vimentin expression (20, 21, 38, 56), the occurrence of MDR3-Pgp is not uniform, but follows a randomly dispersed mosaic pattern. The number of cells expressing the transgene increases from newborn to adult lenses. Therefore, the MDR3-Pgp production, although remaining patchy, can account for the progressive and extensive damages leading to cataract.

The expression of Pgps in eye tissues other than the lens is presumably not the cause of lens damage since during the embryonic stages, the derivatives of ocular connective tissue fully express the transgene or the endogenous Pgps, while the lens displays a normal organization, and its development proceeds unaffected.

Ultrastructural Features of the Lens Expressing MDR3-Pgp

The early ultrastructural alterations in the *MDR*3-Pgp–expressing lens cells are characterized by the presence of cytoplasmic vacuoles of different size and shape, many of them containing internalized membrane profiles and amorphous material. Immunofluorescence and immunogold labeling reveal that the MDR3-Pgp is mainly associated to the plasma membrane outlining the fiber contours and to the membrane-internalized profiles. Moreover, immunoblotting experiments using the antibody raised against P-glycoproteins (mAb C219) demonstrate that MDR3-Pgp is associated to the isolated lens plasma membranes.

At more advanced stages of damage, the inner cortex and the lenticular core show liquefaction areas within the fibers, and the lens is transformed into a cavity comprising cellular debris. The wall of this cavity consists of flattened overlapping cells, with a fully differentiated nuclear and cytoplasmic organization, characterized by a great number of surface projections. Many of these cells express MDR3-Pgp and vimentin. Since they express MP26 too, presumably, they are epithelial cells committed to terminal differentiation and elongation into fibers. Moreover, they are also characterized by membrane domains displaying all different stages of gap junctional assembly characteristic of the process of fiber elongation (2) (Fig. 12, *A* and *C*).

All these data lead us to the conclusion that the expression of MDR3-Pgp in transgenic mouse lenses affects the organization of the plasma membrane, particularly of MP26. This major intrinsic polypeptide of lens fiber membranes (also called MIP or aquaporine) belongs to a superfamily of putative transmembrane channel-forming proteins widespread among living organisms from mammals to bacteria (3, 11, 22). Major functions of this superfamily include the control of water (49, 74, 75) and ion permeability (12, 14, 15, 50). In normal lens fibers and in reconstituted proteoliposomes containing exclusively MP26, the protein forms tetrameric oligomers randomly dispersed in the bilayer (19). Furthermore, the MP26 oligomers can

Figure 9. (*A*) Thin section of cellular elements forming the wall of the lens bladder in an adult cataractous transgenic mouse lens, stained with uranyl acetate and lead citrate. Note the presence of a great number of surface projections and swollen microvilli occupying the membrane surface. (*Inset*) Ultracryosection of the same material incubated with the MP26 antibody. Note that a discrete immunogold labeling outlines the cell surface projections (*arrows*). Bars: (*A*) 1 μm; (*inset*) 125 nm. (*B*) Cryosection of a cataractous adult transgenic mouse lens, immunolabeled with the MP26 antibody. The MP26 fluorescent material is associated either with the plasma membrane or with granular material in the cell cytoplasm. Bar, 50 nm.

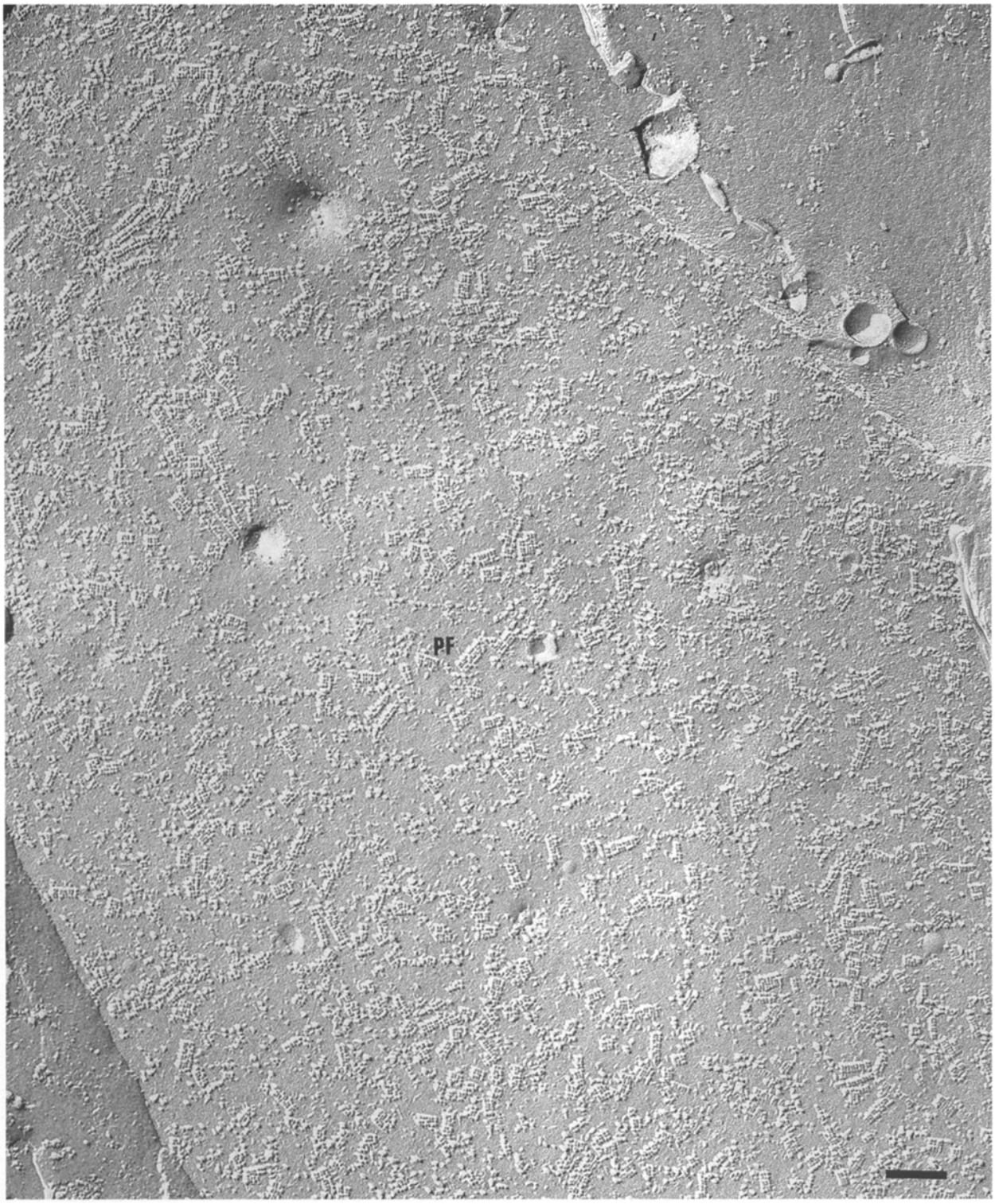

Figure 10. Freeze-fracture replica of a newborn transgenic mouse lens. The protoplasmic fracture face (*PF*) is characterized by a great number of small clusters of square arrays of IMPs. Bar, 120 nm.

form, both in situ and in reconstituted proteoliposomes (19, 46), square arrays of tetrameric subunits. However, in normal lenses, the lattice organization is restricted to the plasma membranes of the nuclear fibers (3, 13, 22, 39, 43). This type of membrane organization has been tentatively correlated with posttranslational degradation of MP26 into MP22 that normally occurs in aged nuclear fibers (3, 13, 22, 39, 43). Square arrays of tetrameric subunits, although to a limited extent, have been described in the nonosmotic hereditary cataract in aged Emory mice, which is a model for senile lens opacification (44, 45, 69).

Our freeze-fracture experiments show that large accu-

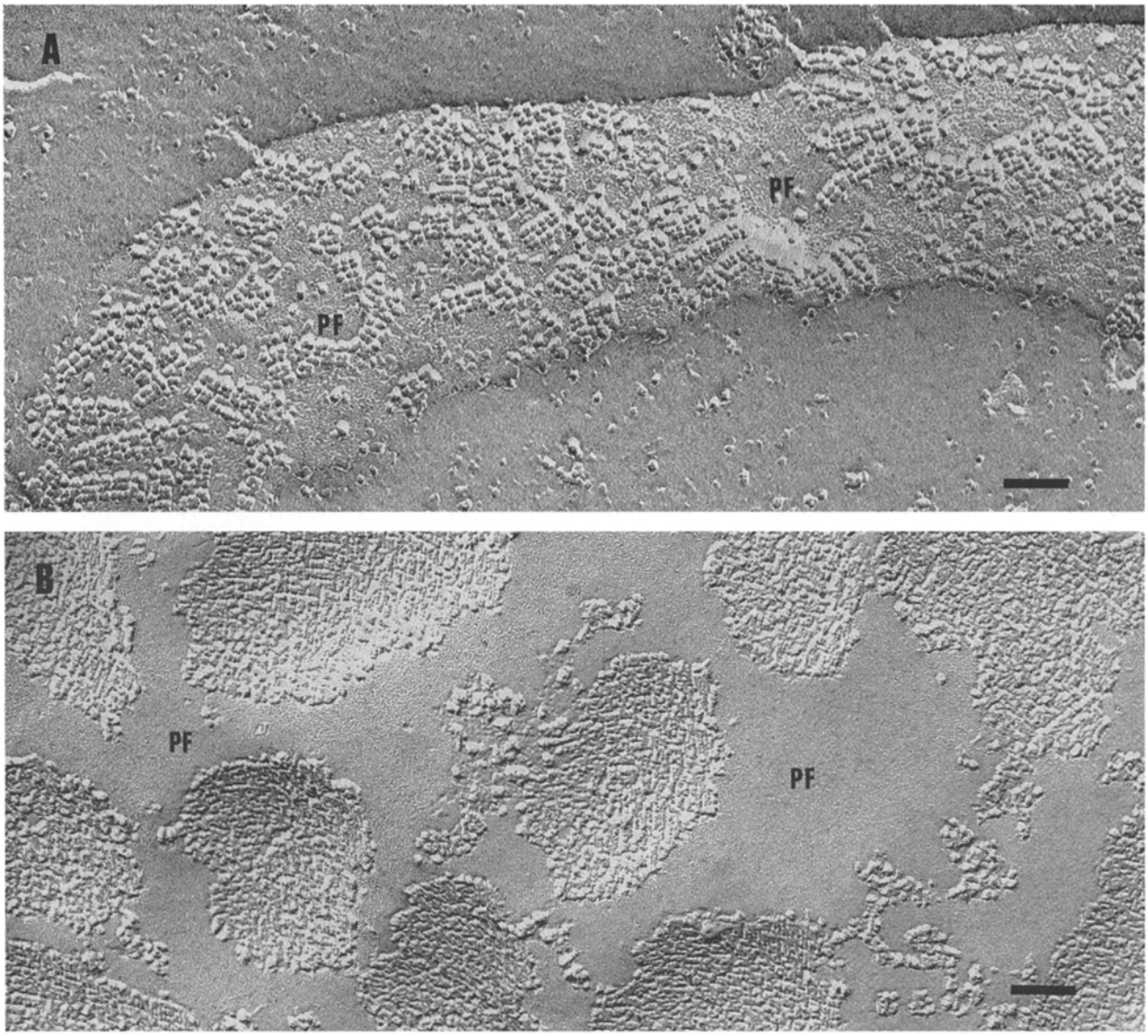

Figure 11. (*A* and *B*) Freeze-fracture replica of a cataractous transgenic mouse lens. (*A*) *PF* fracture faces displaying a great number of square arrays of tetragonal particles. (*B*) IMPs are assembled in large clusters of tetragonally packed repeating subunits, interspaced by areas void of particles. Bars: (*A*) 50 nm; (*B*) 80 nm.

mulations of square arrays of tetrameric subunits are present in cortical fiber plasma membranes of newborn transgenic lenses. This freeze-fracture feature becomes more pronounced in cataractous lenses. The massive appearence of square arrays in *MDR*3 transgenic mouse lenses seems not to be associated with the proteolytic degradation of MP26. This is shown by our immunoblotting experiments using an MP26 antibody. The square array of MP26 tetrameric subunits in *MDR*3 transgenic mouse lens fibers may therefore reflect changes in the membrane lipid environment. Actually, the square lattice, present in the aged nuclear fiber membranes of a normal lens, not only coincides with the posttranslational processing of MP26, but also, if not primarily, with changes of the lipid composition of the plasma membranes. In a normal lens, the aging process of the fiber plasma membranes is characterized by loss of phospholipids, in particular phosphatidylcholine (7, 9, 24). The nuclear fiber membranes contain less than one-third of the concentration of the total phospholipid present in the cortex, with a corresponding increase of the cholesterol/phospholipid ratio (24).

Characteristics of Lens Abnormalities in Transgenic Mouse Lenses

Although cataracts have been described in other transgenic mice, these opacifications lack the characteristic osmotic features of the cataracts in mice overexpressing the *MDR*3 gene. Cataracts generated in lenses overexpressing dominant mutations of intermediate filament genes driven by the vimentin promoter (4, 6, 20, 21) or in transgenic mice overexpressing the retinoic acid receptor protein targeted to the lens by the αA-crystallin promoter (1) lacked a prominent osmotic component. Even overexpression of an ectopic single-pass membrane protein, the H-2D^d major histocompatibility complex class I chain (47), did not induce the distinct alterations of the lens membrane organization observed in *MDR*3 transgenic mice.

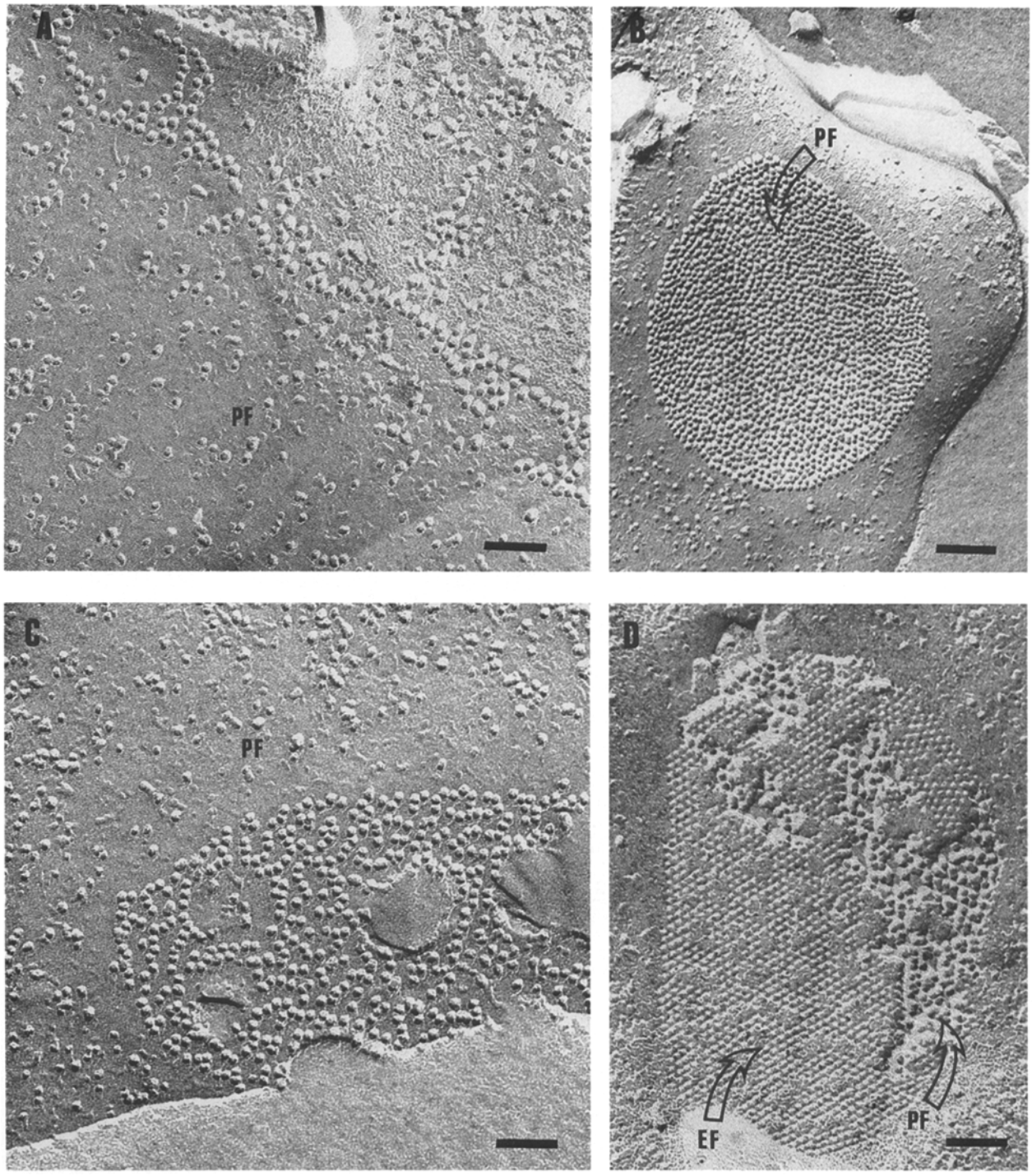

Figure 12. Freeze-fracture replica of a cataractous transgenic mouse lens. (*A* and *C*) The fracture reveals two classes of particles on the *PF*: particles of heterogeneous size between 4 and 7 nm, and 8-nm particles forming linear arrays or clusters. Bar, 70 nm. (*B* and *D*) The fracture reveals macular gap junctions either characterized by a hexagonal array of pitted images on *EF* and geometrical packing of 8-nm particles on *PF* (*D*), or by nongeometrical clusters of 8-nm particles (*B*). Arrows point to *EF* and *PF*, respectively. Bars: (*B*) 120 nm; (*D*) 80 nm.

The ultrastructural abnormalities detected in the lens of newborn and adult transgenic mice expressing the MDR3-Pgp have morphological features in common with those described in the osmotic cataracts of Nakano, Philly, and Fraser (CAT) mice (8, 25, 32, 36, 40, 51, 67, 69, 71). These cataracts develop either during embryonic life or after birth and are characterized by the osmotic swelling of cytoplasmic membrane compartments, internalization of membrane profiles, and liquefaction of the lenticular core. The osmotic cataract in Nakano mice is characterized by the presence of a protein factor that inhibits the Na^+,K^+-ATPase and by posttranslational processing of MP26 into MP22 (25–27, 40, 67, 69). In Philly mice, a deletion of four amino acids has been identified in a region nearby the car-

boxyl terminus of βB2-crystallin affecting the assembly and protein–protein interactions of this protein (8). The osmotic cataracts in both Nakano and Philly mice have been tentatively correlated with an accelerated degradation of MP26 (55).

In mice affected by the dominant Fraser mutation (CAT^{Fr}), lens opacification develops ~day 14 of gestation. The swelling of lens fibers correlates with a defect in the ionic balance (36). Furthermore, the mRNA profile of CAT lenses is consistent with a mutation in the mouse MP26 gene, which results in truncation of MP26 mRNA (48, 49, 61–63).

Strikingly, in the three types of congenital osmotic cataracts mentioned, a major feature is either an inherited dominant defective expression or a degradation process of MP26, in addition to other changes in the metabolism of crystallins (8, 36, 40, 51, 76).

Role of MDR3-Pgp Expression in Lens Damage

Several mechanisms can be envisaged by which the expression of MDR3-Pgp might cause the observed abnormalities. The *MDR*3 gene is the human homologue of the mouse *mdr*2 gene, and it has recently been shown that an *MDR*3 transgene can rescue the liver abnormalities in an *mdr*2 (−/−) mouse homozygous for a disruption of the *mdr*2 gene (Smith, A. J., and P. Borst, unpublished observations). The mdr2-Pgp is a phosphatidylcholine translocator that probably acts as a "flippase," transferring phosphatidylcholine from the inner leaflet of the plasma membrane to the outer leaflet (64). In the presence of bile salts (64) or phosphatidylcholine transfer protein (66), the action of the mdr2/MDR3 translocator may promote export of phosphatidylcholine from the cell. In the absence of such a phospholipid acceptor, i.e., in lens fiber cells, no net phospholipid export can be expected (54, 66), but the action of the translocator might still result in an abnormal distribution of phospholipid species between the two leaflets of the plasma membrane. This, in turn, might induce lattice assembly of MP26, affecting the channel properties of this protein. The new vectorial organization of membrane phospholipids might also generate a lipid bilayer configuration promoting membrane fusion, internalization, and budding of surface projections (17), processes identified in the *MDR*3 transgenic lenses. We cannot exclude, however, that the insertion of a bulky glycoprotein into the plasma membrane would in itself be sufficient to disturb the membrane function, even if it had no direct effect on phospholipid distribution. It is conceivable, for instance, that the MDR3-Pgp could modify either the function of gap junction constituents (29, 30, 41) or of active transporters (26, 27).

We gratefully acknowledge the collaboration of Mr. G. Geraud (Institut Jacques Monod, Paris, France) for the confocal microscopical analysis of our samples. We are also grateful to Mr. M. Recouvreur (Institut Jacques Monod) for the freeze-fracture experiments. We thank Drs. C. Feltkamp and A.H. Schinkel (Netherlands Cancer Institute, Amsterdam, The Netherlands) for advice and help.

The studies of the authors were supported by a European Union Concerted Action on the role of cells membranes in aging and cataract (BMH1-CT93-1650), by the Alcon Research Institute awards to E.L. Benedetti and H. Bloemendal, by the Netherlands Organization for Scientific Research, through the Foundation for Chemical Research to H. Bloemendal, by the French Association against Cancer contract No. 6767, by the French National Research Council and its International Cooperation Department, and by grants NKI 88-6 and NKI 92-41 of the Dutch Cancer Research Society for P. Borst.

Received for publication 4 August 1995 and in revised form 11 October 1995.

References

1. Balkan, W., G.K. Klintworth, C.B. Bock, and E. Linney. 1992. Transgenic mice expressing a constitutively active retinoic acid receptor in the lens exhibit ocular defects. *Dev. Biol.* 151:622–625.
2. Benedetti, E.L., I. Dunia, and H. Bloemendal. 1974. Development of junctions during differentiation of lens fibers. *Proc. Natl. Acad. Sci. USA.* 71: 5073–5078.
3. Benedetti, E.L., I. Dunia, S. Manenti, and H. Bloemendal. 1989. Biochemical and structural properties of the protein constituent of junctional domains in eye lens fiber plasma membranes. *In* Communication and Signalling via Cell to Cell Junctions in Plants and Animals. Vol H46. NATO ASI Series. A.W. Robards and L. Lucas, editors. Springer-Verlag, Berlin/ Heidelberg/New York/Tokyo. 35–52.
4. Bloemendal, H. 1991. Disorganization of membranes and abnormal intermediate filament assembly lead to cataract. *Invest. Ophthalmol. & Visual Sci.* 32:445–455.
5. Buschman, E., and P. Gros. 1991. Functional analysis of chimeric genes obtained by exchanging homologous domains of the mouse *mdr*1 and *mdr*2 genes. *Mol. Cell. Biol.* 11:595–603.
6. Capetanaki, Y., S. Smith, and J.P. Heath. 1989. Overexpression of the vimentin gene in transgenic mice inhibits normal lens cell differentiation. *J. Cell Biol.* 109:1653–1664.
7. Cenedella, R.J. 1985. Regional distribution of lipids and phospholipase A2 activity in normal and cataractous rat lens. *Curr. Eye Res.* 4:113–120.
8. Chambers, C., and P. Russell. 1991. Deletion mutation in an eye lens β-crystallin. *J. Biol. Chem.* 266:6742–6746.
9. Chandrasekher, G., and R. Cenedella. 1993. Calcium activated proteolysis and protein modification in the U18666A cataract. *Exp. Eye Res.* 57:737–745.
10. Chen, C.J., J.E. Chin, K. Ueda, D.P. Clark, I. Pastan, M.M. Gottesman, and I.B. Roninson.1986. Internal duplication and homology with bacterial transport proteins in the *mdr*1 (P-glycoprotein) gene from multidrug-resistant human cells. *Cell.* 47:381–389.
11. Chepelinsky, A.B. 1994. The MIP transmembrane channel family. *In* Handbook of Membrane Channels: Molecular and Cellular Physiology. C. Peracchia, editor. Academic Press, San Diego. 413–432.
12. Chrispeels, M. J., and P. Agre. 1994. Aquaporins: water channel proteins of plant and animal cells. *Trends Biochem. Sci.* 19:421–425.
13. Costello, M.J., T.J. Mcintosh, and D. Robertson. 1989. Distribution of gap junctions and square array junctions in the mammalian lens. *Invest. Ophthalmol. & Visual Sci.* 30:975–989.
14. Deen, P.M.T., M.A.J. Verdijk, N.V.A.M. Knoers, B. Wieringa, L.A.H. Monnens, C.H. van Os, and B.A. van Oost. 1994. Requirement of human renal water channel aquaporin-2 for vasopressin-dependent concentration of urine. *Science (Wash. DC).* 264:92–95.
15. Denker, B.M., B.L. Smith, F.P. Kuhajda, and P. Agre. 1988. Identification, purification and partial characterization of a novel Mr28,000 integral membrane protein from erythrocytes and renal tubules. *J. Biol. Chem.* 263:15634–15642.
16. Devault, A., and P. Gros. 1990. Two members of the mouse *mdr* gene family confer multidrug resistance with overlapping but distinct drug specificities. *Mol. Cell. Biol.* 10:1652–1663.
17. Devaux, Ph. 1992. Protein involvement in transmembrane lipid asymmetry. *Annu. Rev. Biophys. Biomol. Struct.* 21:417–439.
18. Devine, S.E., V. Ling, and P. W. Melera. 1992. Amino acid substitutions in the sixth transmembrane domain of P-glycoprotein alter multidrug resistance. *Proc. Natl. Acad. Sci. USA.* 89:4564–4568.
19. Dunia, I., S. Manenti, A. Rousselet, and E.L. Benedetti. 1987. Electron microscopic observations of reconstituted proteoliposomes with the purified major intrinsic membrane protein of eye lens fibers. *J. Cell Biol.* 105: 1679–1689.
20. Dunia, I., F.R. Pieper, S. Manenti, A. van de Kemp, G. Devilliers, E.L. Benedetti, and H. Bloemendal. 1990. Plasma membrane-cytoskeleton damage in eye lenses of transgenic mice expressing desmin. *Eur. J. Cell Biol.* 53:59–74.
21. Dunia, I., A. van de Kemp, F. Pieper, H. Bloemendal, and E.L. Benedetti. 1991. Eye lens structural abnormalities in mice expressing transgenes affecting the organization of intermediate filaments. *In* Eye Lens Membrane and Aging. Topics in Aging Research, Europe. Vol. 15. G.F.J.M. Vrensen and J. Clauwaert, editors. EURAGE, Leiden. 145–159.
22. Ehring, G.R., G.A. Zampighi, and J.E. Hall. 1993. Does MIP play a role in cell-cell communication? *In* Progress in Cell Research. J.E. Hall, G.A. Zampighi, and R.M. Davis, editors. Elsevier Science Publishers BV, Amsterdam. 153–162.
23. Endicott, J.A., and V. Ling. 1989. The biochemistry of P-glycoprotein-

mediated multidrug resistance. *Annu. Rev. Biochem.* 58:137–171.
24. Fleshner, C.R., and R.J. Cenedella. 1991. Lipid composition of lens plasma membrane fractions enriched in fiber junctions. *J. Lipid Res.* 32:45–53.
25. Fukui, H.N., L.O. Merola, and H. Kinoshita. 1978. A possible cataractogenic factor in the Nakano mouse lens. *Exp. Eye Res.* 26:477–485.
26. Garner, M.H. 1994. Na^+,K^+-ATPases of the lens epithelium and fiber cell: formation of catalytic cycle intermediates and Na^+:K^+ exchange. *Exp. Eye Res.* 58:705–718.
27. Garner, M.H., and J. Horwitz. 1994. Catalytic subunit isoforms of mammalian lens Na, K-ATPase. *Curr. Eye Res.* 13:65–77.
28. Georges, E., G. Bradley, J. Gariepy, and V. Ling. 1990. Detection of P-glycoprotein isoforms by gene-specific monoclonal antibodies. *Proc. Natl. Acad. Sci. USA.* 87:152–156.
29. Gilula, N.B., M. Nishi, and N. Kumar. 1992. Gap junctional communication during mouse development. *In* Advances in Developmental Biology. Vol. 1. P.M. Wassarman, editor. JAI Press, Greenwich, CT. 163–182.
30. Goodenough, D.A. 1992. The crystalline lens. A system networked by gap junctional intercellular communication. *Semin. Cell Biol.* 3:49–58.
31. Gottesman, M.M., and I. Pastan. 1993. Biochemistry of multidrug resistance mediated by the multidrug transporter. *Annu. Rev. Biochem.* 62: 385–427.
32. Graw, J., J. Kratochvilova, and K.H. Summer. 1984. Genetical and biochemical studies of a dominant cataract mutant in mice. *Exp. Eye Res.* 39: 37–45.
33. Gros, P., J. Croop, and D. Housman. 1986. Mammalian multidrug resistance gene: complete cDNA sequence indicates strong homology to bacterial transport proteins. *Cell.* 47:371–380.
34. Gros, P., Y.B. Neriah, J.M. Croop, and D.E. Housman. 1986. Isolation and expression of a cDNA (*mdr*) that confers multidrug resistance. *Nature (Lond.).* 323:728–731.
35. Gros, P., M. Raymond, J. Bell, and D. Housman. 1988. Cloning and characterization of a second member of the mouse *mdr* gene family. *Mol. Cell. Biol.* 8:2770–2778.
36. Haloui, Z., J.P. Pujol, P. Galera, Y. Courtois, and M. Laurent. 1990. Analysis of lens protein synthesis in a cataractous mutant mouse: the Cat Fraser. *Exp. Eye Res.* 51:487–494.
37. Higgins, C.F. 1992. ABC transporters: from microorganisms to man. *Annu. Rev. Cell Biol.* 8:67–113.
38. Kasper, M., and Ch. Viebahn. 1992. Cytokeratin expression and early lens development. *Anat. Embryol.* 186:285–290.
39. Kistler, J., and S. Bullivant. 1980. Lens gap junctions and orthogonal arrays are unrelated. *FEBS (Fed. Eur. Biochem. Soc.) Lett.* 111:73–78.
40. Kobayashi, S., M. Kasuya, and M. Itoi. 1989. Changes in lens proteins induced at the early stage of cataractogenesis in cac (Nakano) mice. *Exp. Eye Res.* 49:553–559.
41. Kumar, N., and N.B. Gilula. 1992. Molecular biology and genetics of gap junctions channels. *Semin. Cell Biol.* 3:3–16.
42. Lincke, C.R., A.M. Van der Bliek, G.J. Schuurhuis, T. van der Velde-Koerts, J.J.M. Smit, and P. Borst. 1990. Multidrug resistance phenotype of human BRO melanoma cells transfected with a wild-type human mdr1 complementary DNA. *Cancer Res.* 50:1779–1785.
43. Lo, W.K., and C.V. Harding. 1984. Square arrays and their role in ridge formation in human lens fibers. *J. Ultrastruc. Res.* 86:228–245.
44. Lo, W.K., and J.F.R. Kuck. 1987. Alterations in fiber cell membranes of Emory mouse cataract: a morphological study. *Curr. Eye Res.* 6:433–444.
45. Lo, W.K., and J.F.R. Kuck. 1990. Alterations of urea-insoluble membrane fraction, MP26, of Emory mouse lenses in aging and cataractogenesis. *Ophthalmic Res.* 22:82–88.
46. Manenti, S., I. Dunia, M. le Maire, and E.L. Benedetti. 1988. High-performance liquid chromatography of the main polypeptide (MP26) of lens fiber plasma membranes solubilized with n-octyl β-D-glucopyranoside. *FEBS (Fed. Eur. Biochem. Soc.) Lett.* 233:148–152.
47. Martin, W.D., R.M. Egan, J.L. Stevens, and J.G. Woodward. 1995. Lens-specific expression of a major histocompatibility complex class I molecule disrupts normal lens development and induces cataracts in transgenic mice. *Invest. Ophthalmol. & Visual Sci.* 36:1144–1154.
48. Muggleton-Harris, A.L., M.F.W. Festing, and M. Hall. 1987. A gene location for the inheritance of the Cataract Fraser (Cat^{Fr}) mouse congenital cataract. *Genet. Res.* 49:235–238.
49. Mulders, S.M., G.M. Preston, P.M.T. Deen, W.B. Guggino, C.H. van Os, and P. Agre. 1995. Water channel properties of major intrinsic protein of lens. *J. Biol. Chem.* 270:1–7.
50. Nielsen, S., B.L. Smith, E.I. Christensen, and P. Agre. 1993. Distribution of the aquaporin CHIP in secretory and resorptive epithelia and capillary endothelia. *Proc. Natl. Acad. Sci. USA.* 90:7275–7279.
51. Piatigorsky, J. 1980. Differential synthesis and degradation of protein in the hereditary Philly mouse cataract. *Exp. Eye Res.* 30:69–78.
52. Pieper, F.R., G. Schaart, P.J. Krimpenfort, J.B. Henderik, H.J. Moshage, A. van de Kemp, F.C. Ramaekers, A. Berns, and H. Bloemendal. 1989. Transgenic expression of the muscle-specific intermediate filament protein desmin in nonmuscle cells. *J. Cell Biol.* 108:1009–1024.
53. Ramaekers, F.C.S., J.J.G. Puts, O. Moesker, A. Kant, A. Huysmans, D. Haag, P.H.K. Jap, C. Herman, and G.P. Vooijs. 1983. Antibodies to intermediate filament proteins in the immunohistochemical identification of human tumours: an overview. *Histochem. J.* 15:691–713.
54. Ruetz, S., and P. Gros. 1994. Phosphatidylcholine translocase: a physiological role for the mdr2 gene. *Cell.* 77:1071–1081.
55. Russel, P. 1981. Changes in intrinsic membrane proteins in mouse lens during cataractogenesis. *In* New Directions in Ophthalmic Research. M.L. Sears, editor. Yale University Press, New Haven, CT. 109–121.
56. Sax, C.M., F.X. Farrell, Z.E. Zehner, and J. Piatigorsky. 1990. Regulation of vimentin gene expression in the ocular lens. *Dev. Biol.* 139:56–64.
57. Schinkel, A.H., and P. Borst. 1991. Multidrug resistance mediated by P-glycoproteins. *Semin. Cancer Biol.* 2:213–226.
58. Schinkel, A.H., M.E.M. Roelofs, and P. Borst. 1991. Characterization of the human MDR3 P-glycoprotein and its recognition by P-glycoprotein-specific monoclonal antibodies. *Cancer Res.* 51:2628–2635.
59. Schinkel, A.H., R.J. Arceci, J.J.M. Smit, E. Wagenaar, F. Baas, M. Doll, T. Tsuruo, E.B. Mechetner, I.B. Roninson, and P. Borst. 1993. Binding properties of monoclonal antibodies recognizing external epitopes of the human MDR1 P-glycoprotein. *Int. J. Cancer.* 55:478–484.
60. Schinkel, A.H., J.J.M. Smit, O. van Tellingen, J.H. Beijnen, E. Wagenaar, L. van Deemter, C.A.A.M. Mol, M.A. van der Valk, E.C. Robanus-Maandag, H.P.J. te Riele, et al. 1994. Disruption of the mouse mdr1a P-glycoprotein gene leads to deficiency in the blood-brain barrier and to increased sensitivity to drugs. *Cell.* 77:491–502.
61. Shiels, A., and C.S. Griffin. 1993. Aberrant expression of the gene for lens major intrinsic protein in the CAT mouse. *Curr. Eye Res.* 12:913–921.
62. Shiels, A., C.S. Griffin, and A.L. Muggleton-Harris. 1991. Immunochemical comparison of the major intrinsic protein of eye-lens fibre cell membranes in mice with hereditary cataracts. *Biochim. Biophys. Acta.* 1097: 318–324.
63. Shiels, A., C.S. Griffin, and A.L. Muggleton-Harris. 1991. Restriction fragments length polymorphisms associated with the gene for the major intrinsic protein of eye-lens fibre cell membranes in mice with hereditary cataracts. *Biochim. Biophys. Acta.* 1097:81–85.
64. Smit, J.J.M., A.H. Schinkel, R.P.J. Oude Elferink, A.K. Groen, E. Wagenaar, L. van Deemter, C.A.A.M. Mol, R. Ottenhoff, N.M.T. van der Lugt, M.A. van Roon, et al. 1993. Homozygous disruption of the murine *mdr2* P-glycoprotein gene leads to a complete absence of phospholipid from bile and to liver disease. *Cell.* 75:451–462.
65. Smit, J.J.M., A.H. Schinkel, C.A.A.M. Mol, D. Majoor, W.J. Mooi, A.P.M. Jongsma, C.R. Lincke, and P. Borst. 1994. The tissue distribution of the human MDR3 P-glycoprotein. *Lab. Invest.* 71:638–649.
66. Smith, A.J., J.L.P.M. Timmermans-Hereijgers, B. Roelofsen, K.W.A. Wirtz, W.J. van Blitterswijk, J.J.M. Smit, A.H. Schinkel, and P. Borst. 1994. The human MDR3 P-glycoprotein promotes translocation of phosphatidylcholine through the plasma membrane of fibroblasts from transgenic mice. *FEBS (Fed. Eur. Biochem. Soc.) Lett.* 354:263–266.
67. Tekehana, M. 1990. Hereditary cataract of the Nakano mouse. *Exp. Eye Res.* 50:671–676.
68. Tokuyasu, K.T. 1983. Present status state of immuno-ultracryomicrotomy. *J. Histochem. Cytochem.* 31:264–274.
69. Tripathi, B.J., R.C. Tripathi, N.S.C. Borisuth, R. Dhaliwal, and D. Dhaliwal. 1991. Rodent models of congenital and hereditary cataract in man. *Lens and Eye Toxicity Research.* 8:373–413.
70. Ueda, K., C. Cardarelli, M.M. Gottesman, and I. Pastan. 1987. Expression of a full-length cDNA for the human "MDR1" gene confers resistance to colchicine, doxorubicin, and vinblastine. *Proc. Natl. Acad. Sci. USA.* 84: 3004–3008.
71. Uga, S., P.F. Kador, and T. Kuwabara. 1980. Cytological study of Philly mouse cataract. *Exp. Eye Res.* 30:79–92.
72. van der Bliek, A.M., F. Baas, T. Ten Houte de Lange, P.M. Kooiman, T. van der Velde-Koerts, and P. Borst. 1987. The human mdr3 gene encodes a novel P-glycoprotein homologue and gives rise to alternatively spliced mRNAs in liver. *EMBO (Eur. Mol. Biol. Organ.) J.* 6:3325–3331.
73. van der Bliek, A.M., P.M. Kooiman, C. Schneider, and P. Borst. 1988. Sequence of mdr3 cDNA encoding a human P-glycoprotein. *Gene (Amst.).* 71:401–411.
74. van Os, C.H., P.M.T. Deen, and J.A. Dempster. 1994. Aquaporins: water selective channels in biological membranes. Molecular structure and tissue distribution. *Biochim. Biophys. Acta.* 1197:291–309.
75. Verbavatz, J.-M., D. Brown, I. Sabolić, G. Valenti, D.A. Ausiello, A.N. Van Hoek, T. Ma, and A.S. Verkman. 1993. Tetrameric assembly of CHIP28 water channels in liposomes and cell membranes: a freeze–fracture study. *J. Cell Biol.* 123:605–618.
76. Zigler, J.S. 1990. Animal models for the study of maturity-onset and hereditary cataract. *Exp. Eye Res.* 50:651–657.